Toward Functional PET Imaging of the Spinal Cord

Pierre Courault, Luc Zimmer, Sophie Lancelot

ELSEVIER

Seminars in
NUCLEAR
MEDICINE

Toward Functional PET Imaging of the Spinal Cord

Pierre Courault, PharmD, PhD,[†,‡,§] Luc Zimmer, PharmD, PhD,[†,‡,§,‖] and Sophie Lancelot, PharmD, PhD[†,‡,§]

At present, spinal cord imaging primarily uses magnetic resonance imaging (MRI) or computed tomography (CT), but the greater sensitivity of positron emission tomography (PET) techniques and the development of new radiotracers are paving the way for a new approach. The substantial rise in publications on PET radiotracers for spinal cord exploration indicates a growing interest in the functional and molecular imaging of this organ. The present review aimed to provide an overview of the various radiotracers used in this indication, in preclinical and clinical settings. Firstly, we outline spinal cord anatomy and associated target pathologies. Secondly, we present the state-of-the-art of spinal cord imaging techniques used in clinical practice, with their respective strengths and limitations. Thirdly, we summarize the literature on radiotracers employed in functional PET imaging of the spinal cord. In conclusion, we propose criteria for an ideal radiotracer for molecular spinal cord imaging, emphasizing the relevance of multimodal hybrid cameras, and particularly the benefits of PET-MRI integration.

Introduction

The Spinal Cord, Anatomy, Neurophysiology and Neurotransmission

The spinal cord is part of the central nervous system (CNS), located within the spinal canal and protected by the vertebral column. It is comprises 31 spinal nerve pairs: eight cervical, 12 thoracic, five lumbar, five sacral and one coccygeal.[1] Like the rest of the CNS, the spinal cord is composed of gray and white matter. The gray matter is organized around the central canal in an H shape, divided into a ventral and a dorsal horn. The ventral horn contains alpha and gamma motor neurons, while the dorsal horn contains second-order projections and intrinsic neurons. Between the two, there is the intermediolateral column, which contains preganglionic cells of the autonomic nervous system.

Dorsal horn axonal terminals from higher structures such as the brainstem express various neurotransmitters. Several receptors have been identified in the spinal cord and are potential targets. Glutamatergic neurotransmission in the spinal cord exerts its excitatory effect by activating N-methyl-D-aspartate (NMDA) or α-amino-3-hydroxy-5-methylisoxazol-4-proprionate (AMPA) receptors, which are ionotropic receptors.[2] Inhibition of the CNS is mediated by γ-aminobutyric acid (GABA) and glycine.[3] These neurotransmitters target respectively the glycine and $GABA_A$ receptors, which are chloride channels. Monoamine neurotransmitters such as serotonin (5-HT) or dopamine (DA) and their receptors, $5\text{-}HT_{1A/2A}$ and D2/D3 respectively,[4,5] have been widely reported to be involved in modulating neural information processing. Acetylcholine and adrenergic neurotransmitters (epinephrine and norepinephrine) are also found in spinal cord neurotransmission. Acetylcholine binds to its nicotinic receptor, while epinephrine and norepinephrine bind to α-adrenergic receptors.[6] Neuropeptides such as substance P or calcitonin gene related peptide (CGRP) also regulate neuronal information and bind to their related receptors, neurokinin 1 (NK1) and CGRP receptor respectively.[7,8] All this

[†]Lyon Neuroscience Research Center (CRNL), INSERM, CNRSx, Lyon, France.
[‡]Hospices Civils de Lyon (HCL), Lyon, France.
[§]CERMEP-Imaging Platform, Lyon, France.
[‖]National Institute for Nuclear Science and Technology (INSTN), CEA, Saclay, France.
Address reprint requests to Luc Zimmer CERMEP, Groupement Hospitalier Est, 59 Boulevard Pinel, F-69500 Bron, France. E-mail: luc.zimmer@univ-lyon1.fr

https://doi.org/10.1053/j.semnuclmed.2024.07.002

neuroanatomy is important to consider, as it gives numerous potential targets for spinal cord positron emission tomography (PET) imaging.

Spinal Cord Pathologies

Spinal Cord Injury

Spinal cord injury results from trauma or spinal cord disease. Even if the spinal cord is not entirely disrupted, spinal cord injury can trigger functional and motor disabilities accompanied by social issues.[9] Worldwide, the World Health Organization estimates that between 250,000 and 500,000 people suffer from spinal cord injury. Magnetic resonance imaging (MRI) and computed tomography (CT) play an important role in diagnosis of spinal cord injury. In case of soft-tissue injury, MRI is preferable while CT is more suited for fractures.[10] Nowadays, prevention of accidents leading to spinal cord injury and rehabilitation are the most crucial aspects of care. No pharmacological treatment is available for spinal cord recovery.[11]

Multiple Sclerosis

Multiple sclerosis (MS) is a neurodegenerative disease of the CNS that can affect both brain and spinal cord. According to the National Multiple Sclerosis Society, 2.8 million people have MS (https://www.nationalmssociety.org), although distribution varies from one region to another.[12] Pathophysiology may involve an autoimmune response mediated by autoreactive lymphocytes entering the CNS, causing inflammation resulting in demyelination and neuron loss.[13] Diagnosis is first based on clinical presenting symptoms, which may be difficult to identify depending on whether the disease is relapsing or progressive.[14] When MS is suspected, MRI is recommended to highlight brain abnormality, present in 80% of patients. Examination of cerebrospinal fluid is also indicative but not strictly necessary. Final diagnosis is based on the 2017 McDonald criteria.[15] There is no treatment to stop the development of the disease, but available treatments can either reduce the severity of MS episodes or slow progression and manage symptoms.[16]

Amyotrophic Lateral Sclerosis

Amyotrophic lateral sclerosis (ALS) is a neurodegenerative disease with progressive nerve loss in brainstem, motor cortex and spinal cord, impairing muscle control. Between 1 and 2.6 cases per 100,000 persons are diagnosed annually and prevalence is around six per 100,000.[17] Clinical features are characterized by progressive muscle weakness, spasticity and respiratory failure, causing death 3-5 years after symptom onset.[18] As there is no specific diagnostic test, diagnosis is based on history, clinical symptoms, electroneuromyography and exclusion of other neurodegenerative diseases.[19] A genetic test is also proposed, to distinguish a familial from sporadic disease. Two drugs have been approved for ALS treatment: riluzole and edaravone.[20,21]

Neuropathic Pain

Neuropathic pain (NP) is defined as a pain caused by somatosensory system damage, with a prevalence around 5%-7%.[22] Diagnosis is based only on the patient's experience and is purely subjective. Management focuses on symptoms, as the cause is generally not known. Many drugs, such as pregabalin or tricyclic antidepressants, have been used but showed variable efficacy, and patients are frequently left without any effective option.[23] Due to its role in neuromodulation of pain, the spinal cord is frequently suggested as a target for treatment.

Huntington's Disease

Huntington's disease (HD) is neurodegenerative disease which affects motor, cognitive and behavioral functions. It is a genetic autosomal-dominant disease which leads to a mutated protein named huntingtin.[24] Incidence is 0.38 per 100,000 per year and world-wide prevalence is estimated at 2.71 per 100,000, with lower incidence and prevalence in Asia than in other continents.[25] Diagnosis is first based on clinical symptoms, of which Huntington's chorea and dystonia are the most significant. Secondly, diagnosis is highlighted by genetic mutation of an expanded CAG repeat on exon one of the gene encoding for huntingtin protein.[26] Multidisciplinary care combines pharmacological treatment with other specialties (physiotherapy, psychology, speech pathology).[27,28] Pharmacological treatment aims to reduce psychiatric symptoms (antidepressants, anxiolytics, etc.) and chorea symptoms (dopamine-depleting agents, antipsychotics, etc.).[29] Sciacca and Cicchetti recently reported the presence of mutant huntingtin protein in the spinal cord due to impairment of the blood-spinal-cord barrier (BSCB).[30] This suggests an important role for therapeutics.

Lumbar Radiculopathy

Radiculopathies are due to the compression of nerve roots at various levels of the spinal cord: cervical, thoracic, lumbar, or sacral. The prevalence of lumbar radiculopathy is 3%-5%.[31] Diagnosis is based on history and physical examination, and can be confirmed by MRI, which may show root compression.[32] In case of discrepancy between MRI and clinical findings, electrodiagnosis can be useful. Treatment is nonsurgical, with physical exercises, and pharmacological treatment with nonsteroidal anti-inflammatory drugs in first line, orally and then by injection.[33] Surgical treatment can be proposed when nonsurgical treatment is not sufficient.[32]

Spinal Cord Visualization

Magnetic Resonance Imaging

MRI is used for spinal cord imaging in several indications: spinal cord injury or multiple sclerosis.[34,35] It provides different fields of information depending on the sequences used. Classic anatomical MRI sequences give information on the structure and integrity of the spinal cord.[36] Functional MRI (fMRI) records the blood-oxygenation-level-dependent (BOLD) signal and thus gives information on neuronal activation in the

spinal cord.[37] Diffusion tensor imaging uses interactions of protons in water to image white-matter fibers in the spinal cord,[38] providing microstructural information on fiber direction, as the spinal cord is structured anisotropically. MR spectroscopy quantifies metabolic and biochemical structures in the spinal cord.[39] MRI also has the advantage of not involving radiation for the patient. Finally, enhancement of MRI performance from 1.5 to three or seven Tesla has improved image resolution,[40] which is particularly important as the spinal cord is a fine structure. MRI has several strengths in spinal cord imaging. Firstly, it is nonirradiating, unlike PET or CT. It has better contrast resolution in soft tissue such as spinal cord. It can be used in anatomical or functional modalities, with many different sequences. Basic sequences comprise fast spin echo T2 and spin echo T1; more advanced sequences can provide further information, such as diffusion tensor imaging, angio-dynamic MRI, spectroscopy or short tau inversion recovery.[41] However, spinal cord MRI suffers from several limitations. Firstly, it is nonspecific, as it measures proton signals. The spinal cord has a nonhomogeneous magnetic field, which limits the use of MRI, due to distortion of the image and signal loss.[37] Moreover, the spinal cord is a small structure with microstructural anatomy and thus requires high-resolution imaging. Transverse images are the most accurate slices for the spinal cord, as they have greater spatial resolution; however, this requires more slices to image the complete spinal cord and thus is time-consuming. Plus, spinal cord MRI is hampered by physical movement due to the respiratory and cardiac cycles. Many artifacts occur in some situations, due to cerebrospinal fluid, breathing or patient movements. Finally, quantitative MRI techniques are technically challenging and are limited to certain area of research which are able to implement these techniques.

Computed Tomography

CT is used to image the spinal cord in various pathologies. It is more suitable than MRI for imaging osseous tissue, and is commonly used to assess structural disease[42] and fracture extension after spinal cord injury.[43] It is also used in oncology to detect tumors and metastases or for CT-guided biopsy.[44] CT angiography is used to image spinal vascular malformations.[45] MRI shows higher sensitivity for imaging soft tissue, but CT less time-consuming and less expensive.

Taken together, MRI and CT are important methods providing several types of information on spinal cord integrity. PET imaging is complementary, as it provides molecular information and could be an interesting tool to discover new targets. Below we provide a short review of [^{18}F]fluoro-2-deoxy-D-glucose ([^{18}F]FDG) PET imaging for the spinal cord, as it is widely used clinically. We then explore the new PET radiotracers for spinal cord PET imaging.

[^{18}F]Fluoro-2-Deoxy-D-glucose PET Spinal Cord Imaging

[^{18}F]FDG is a PET radiopharmaceutical widely use to image glucose metabolism in cells. Due to the ubiquitous role of glucose, [^{18}F]FDG is used in several indications. Based on a recent systematic review, the physiological distribution of [^{18}F]FDG in the spinal cord shows uptake all along the spine, decreasing from cervical to thoracic levels. Two uptake peaks were shown in lower cervical (C4-6) and lower thoracic (T12) regions of the spinal cord.[46] Studies also explored the potential of [^{18}F]FDG to image the spinal cord in various pathologies. Firstly, [^{18}F]FDG was used in oncology to image metastasis extending to the spinal cord in patients with lung cancer, lymphoma or glioblastoma.[47-50] Patients with intramedullary myelopathy were also described.[51] [^{18}F]FDG was also used to explore specific spinal cord pathologies to distinguish between malignant and osteoporotic fractures,[52-54] low back pain[55] or sarcoidosis.[56,57] [^{18}F]FDG was proposed to image spinal cord injury, but only in a preclinical model.[58,59] Neurodegenerative diseases which could affect the spinal cord, such as MS[60] or ALS,[61] have also been explored with [^{18}F]FDG and showed interesting results. Other pathologies indirectly affecting the spinal cord, such as cervical gout,[62] have also been explored. [^{18}F]FDG PET spinal cord imaging has been explored in pediatric populations and showed higher uptake in the cervical level (C1-C7), and dorsal and lumbar level (D7-L1).[63]

[^{18}F]FDG is widely used for PET spinal cord imaging as it has market authorization and is used worldwide by almost every nuclear medicine center. As described above, [^{18}F]FDG PET is an interesting tool for differential diagnosis between osteoporotic and malignant fractures.[53,54] It can also distinguish spinal cord tumor infiltrate from inflammatory disease.[64] However, this indication may give way to new PET radiopharmaceuticals targeting specific inflammatory proteins (see below). PET is also useful in case of contraindications to MRI, which is the main modality for spinal cord exploration. Finally, in a multimodal approach [^{18}F]FDG PET could be complementary to other techniques when patients show normal MRI or CT but with high clinical suspicion of spinal cord disease. Some case reports described the use of [^{18}F]FDG PET in complement to other modalities to help in differential diagnosis.[56,62,65]

[^{18}F]FDG PET spinal cord imaging has some limitations. First, glucose metabolism is not specific to the spinal cord or spinal disease. In inflammatory disease, radiopharmaceutical uptake could reflect either spinal cord inflammatory response or an inflammatory process from surrounding tissue.[66] Moreover, [^{18}F]FDG can be influenced by glucose metabolic activity or glucocorticoids, which are commonly used in the spinal cord pathologies such as MS or spinal cord injury. Different confounding factors affect interpretation of [^{18}F]FDG spinal cord PET images. For example, age showed mixed results, with negative,[67] positive[68] or no correlation.[69] Other factors such as female gender and greater body weight also showed variable correlation with [^{18}F]FDG uptake.[46] Moreover, some tumors have been reported not to be detected by [^{18}F]FDG PET, due to lack of uptake, while being easily seen on MRI.[70] These interactions need to be clarified. Finally, the quantification method for spinal cord uptake needs to be standardized. Studies used SUV or lesion-

to-background SUV ratio, and took different organs or levels of the spinal cord as reference.[71]

PET Radiotracers in Development for Functional Spinal Cord Imaging

TSPO PET Radiotracers

[^{11}C]PK11195

[^{11}C]PK11195 is a widely used PET as first-generation of radiotracer targeting the translocator protein (TSPO) to assess inflammation in various diseases.[72,73] [^{3}H]/[^{11}C]PK11195 was first proposed for spinal cord imaging by Vowinckel et al., as marker of microglial activation in experimental autoimmune encephalomyelitis (EAE) in mice and in MS in patients.[74] In this study, autoradiography using [^{3}H]PK11195 showed specific low-level binding to gray matter in the spinal cord in normal and EAE mice. In EAE mice, high binding was also found within the white matter of inflamed regions. Other autoradiography studies also showed binding differences in the spinal cord in MS and in nerve transection and crush injury models until 4 weeks after injury.[75,76] In patients, [^{11}C]PK11195 showed increased lesion uptake. These results suggested that [^{11}C]PK11195 could be a suitable radiotracer for evaluating spinal cord injury in MS and EAE.

In vivo, [^{11}C]PK11195 was used in an EAE rat model of MS.[77] In this study, [^{11}C]PK11195 was used to image neuroinflammation in the spinal cord while [^{11}C]MeDAS was used for demyelination (see below for the latter). Rats underwent PET/CT scan at baseline and at days 6, 11, 15 and 19 after induction. One animal was sacrificed at each time point for immunohistochemistry to assess myelin density and ionized calcium-binding adapter molecule 1 (Iba-1). Rats were separated in two groups: treated (dexamethasone) and nontreated (saline). [^{11}C]PK11195 in the spinal cord showed significantly increased uptake compared to baseline at day 11 (+41%), day 15 (+49%) and day 19 (+41%) in the saline-treated group. No differences and no increase in uptake were found in the dexamethasone-treated group. In the dexamethasone-treated group, higher [^{11}C]PK11195 uptake was found in the spinal cord in rats that developed symptoms compared to rats that did not (+22%). A strong correlation was found between [^{11}C]PK11195 spinal cord uptake and the Iba-1 biomarker ($r^2 = 0.79$).

[^{11}C]PK11195 was also used by Imamoto et al. in a model of partial sciatic nerve ligation (PSNL) to visualize spinal glial activation.[78] Rats underwent PET/CT scans at 0 (naïve), 7 and 14 days after PSNL. At each time point, some rats were sacrificed and L3-L6 segments were isolated to perform in-vitro [^{11}C]PK11195 spinal cord autoradiography. [^{11}C]PK11195 PET scans showed higher uptake in the lumbar spinal cord at days 7 and 14 after nerve injury and lower uptake in other regions (ie, thoracic). This increase was confirmed to be TSPO-specific using competition assays. [^{3}H]PK11195 autoradiography also confirmed these results and showed greater accumulation in the ipsilateral dorsal horn of the injured nerve. These results correlated strongly with pain (von Frey filament test), microglia marker (CD11b and Iba-1) elevation and, to a lesser extent, with astrocyte marker (GFAP) elevation.

[^{18}F]DPA-714

[^{18}F]DPA-714 is a second-generation PET radioligand for the TSPO. Abourbeh et al. used [^{18}F]DPA-714 to explore microglial activation in the spinal cord in a model of induced EAE.[79] PET/CT scans were performed 10-12 days after EAE induction. Two types of PET reconstruction were performed: 2D ordered-subset expectation maximization (2D-OSEM), and 3D-OSEM maximum a-posteriori estimation (FMAP). Biodistribution study and Western blot analysis were also performed. In-vivo PET imaging showed 2.6-fold greater uptake in the spinal cord in EAE rats than in controls. For reconstruction, FMAP showed uptake values closer to the ex-vivo biodistribution than 2D-OSEM. Biodistribution study also showed four to five-fold greater uptake in the spinal cord in EAE rats than control rats. Higher uptake was also found in the lumbar than the thoracic level. Competition study confirmed the specificity of this binding, in-vivo and ex-vivo. TSPO-expression in EAE rats was also five-fold higher than in controls. Spinal cord immunostaining confirmed colocalization of microglia/macrophage activation, rather than astrocytes.

Gargiulo et al. also used [^{18}F]DPA-714 to image microglial activation in the spinal cord (and brain) in a mouse model of ALS.[80] Transgenic SOD1^{G93A} and wild type (WT) SOD1 control mice underwent PET/CT scans with [^{18}F]DPA-714 to evaluate, among other things, cervical spinal cord binding. Immunochemistry was also performed all along the spinal cord after collection, and divided into cervical, thoracic and lumbar sections. Visual analysis of in-vivo PET images showed higher [^{18}F]DPA-714 uptake in the cervical spinal tract of SOD1^{G93A} mice than WT SOD1 mice. However, this 1.6-fold increase in uptake (3.243 ± 1.409 vs 2.084 ± 0.551 for SOD1^{G93A} and WT SOD1 respectively) was not significant. On immunochemistry, the cervical thoracic and lumbar microglial marker (Iba-1) was elevated in SOD1^{G93A} mice, and colocalized with TSPO-expression.

Shimochi et al. performed [^{18}F]DPA-714 PET/CT imaging in a rat model of NP to detect microglia activation in the spinal cord.[81] [^{18}F]DPA-714 was compared to [^{11}C]PK11195. The model consisted of a PSNL model and control rats received sham surgery. In-vivo PET/CT imaging were performed on day 7 and rats were sacrificed for autoradiography, biodistribution study, immunohistochemical staining and ex-vivo PET imaging of the spinal cord. Two types of PET/CT scanner were used for [^{18}F]DPA-714 imaging: Molecubes or Inveon. Autoradiography showed preferential accumulation in the ipsilateral dorsal and ventral horns of the lumbar spinal cord, colocalized with immunostaining of Iba-1 microglial activation marker. Ipsi-/contra-lateral lumbar ratios were significantly higher for [^{18}F]DPA-714 (2.91 ± 0.47) than [^{11}C]PK11195 (1.78 ± 0.34) and were also higher in experimental than control rats for [^{18}F]DPA-714 .

Blocking study confirmed the specific binding of each radiotracer. Ex-vivo imaging of the PSNL model showed higher uptake of [^{18}F]DPA-714 in the inflammation site next to the lumbar spinal cord than in sham animals and the reference thoracic level. Lesion-to-background ratio was also higher with [^{18}F]DPA-714 than [^{11}C]PK11195. On in-vivo imaging, no differences were found between lumbar and thoracic regions for either radiotracer. These results were not consistent with previous studies of [^{11}C]PK11195, which showed higher uptake in injured regions of the spinal cord.[78] These conflicting results may be attributed to the small lesion site and insufficient SUV relative to background.

[^{11}C]PBR28

[^{11}C]PBR28 is a second-generation TSPO PET radiotracer. One clinical study used [^{11}C]PBR28 in a spinal cord indication to assess immunoactivation in lumbar radiculopathy.[82] Participants were patients suffering from radicular pain (n = 16) and healthy control subjects (n = 10). Interestingly, participants underwent 90 minutes PET-MRI scans, in contrast to studies using PET/CT scans. Patients were treated by epidural steroid injection, after (n = 7) or before PET-MRI scans. Spinal cord [^{11}C]PBR28 uptake was measured in a "target region" (T11-T12 thoracic vertebrae, which contain the sciatic nerve) and a "reference region" (T7-T9). Results showed significantly higher uptake in the target than in the reference region or in healthy controls. The [^{11}C]PBR28 uptake ratio between target and reference neuroforamina was associated with epidural steroid injection response. This study suggested that central immune response could be an interesting target to treat lumbar radiculopathy, and preselecting patients using the [^{11}C]PBR28 neuroforamen ratio could improve care.

[^{18}F]GE-180

[^{18}F]GE-180 is a third-generation of TSPO PET radiotracer binding with high affinity to its target.[83,84] Tremoleda et al. developed a model of spinal cord injury by contusion at level T10 in rats.[85] Control groups were either naïve or with laminectomy. The therapeutic effect of docosahexaenoic acid (DHA) was also assessed in a subgroup (SCI-DHA) vs saline injection (SCI-saline). In-vivo [^{18}F]GE-180 PET/CT imaging was performed at day 7 after surgery. Biodistribution, ex-vivo autoradiography and histology analysis were also performed after sacrifice. Results showed higher uptake in T10 in the spinal cord injury group (0.55 ± 0.2 %ID/g) than in the naïve group (0.35 ± 0.2 %ID/g) or the laminectomy group (0.29 ± 0.06 %ID/g): ie 1.4- and 1.9-fold increases. No differences were found in other regions of the spinal cord. The biodistribution study confirmed the preferential radiotracer uptake at T10 level compared to other regions in the spinal cord injury group (0.85 ± 0.3 %ID/g vs 0.25 ± 0.04 %ID/g). This difference was not found in the naïve or laminectomy group. In the treated group, DHA showed a trend for lower radiotracer uptake in-vivo, but without significant difference (20% higher uptake in the SCI-saline than in the SCI-DHA group). Biodistribution study also showed lower T10 uptake in the SCI-DHA than the SCI-saline group. However, there were no differences between T10 and other regions in the SCI-DHA group. Autoradiography analysis confirmed these results. Immunochemistry analyses also correlated with the radiotracer analysis and showed respectively 1.3 and 6.0-fold greater TSPO-expressing cell levels at T10 in the spinal cord injury group than in the laminectomy and naïve groups. TSPO expression was lower in the SCI-DHA than in the SCI-saline subgroup (26 % vs 40% respectively). Finally, increased Iba-1 expression indicated a response mediated by microglial cells, while GFAP (astrocytes) showed no increase.

Cropper et al. used [^{18}F]GE-180 to assess central and peripheral microglial activation in a model of complex regional pain syndrome (CRPS).[86] In this study, mice underwent PET/CT imaging at days 2, 7 and 21 and weeks 7 and 20 after CRPS surgery. Ex-vivo biodistribution, autoradiography and TSPO-expression immunochemistry studies were also performed to confirm in-vivo imaging. Dynamic in-vivo PET/CT showed increased uptake of [^{18}F]GE-180 in the spinal cord for the CRPS group during the acute phase (days 7 to 21) at cervical/thoracic level (around 1.25-fold) and lumbar level (around 1.27-fold) but not in the chronic phase (weeks 7-20). Ex-vivo biodistribution and autoradiography studies confirmed these results. Immunochemistry analysis showed increased levels of activated microglia (CD11b) and TSPO-expression colocalization at day 7 in CRPS mice (13% colocalization at baseline vs 57% at day 7). No colocalization was found between TSPO and GFAP astrocyte markers, although both markers were elevated. At week 7, microglia and astrocytes returned to baseline.

[^{11}C]DAC

[^{11}C]DAC is a recently developed PET TSPO radiotracer.[87] One study used it to image the spinal cord in an EAE rat model of MS.[88] Rats underwent PET/CT scans at 0, 7, 11, 20 and 60 days after EAE induction. Three groups were followed up: control, EAE induction and EAE treated with FTY720 (immunosuppressive therapy). Biodistribution study was also performed after sacrifice at each day after PET scans. In-vitro autoradiography was performed at days 0 and 11 in EAE rats. Histological and immunohistochemical analysis assessed inflammation and TSPO expression in various cell types. Dynamic PET spinal cord images showed significantly increased uptake of [^{11}C]DAC at day 11 in EAE rats compared to controls. An increase was also detected at days 7 and 20 (start of remission). These results were consistent in thoracic, lumbar and sacral spinal cord levels. [^{11}C]DAC uptake was markedly greater in the un-treated compared to the treated group. In-vitro autoradiography and biodistribution study confirmed specific TSPO labeling by [^{11}C]DAC. These results were also consistent with inflammation exploration. Immunohistochemical analysis showed overexpression of TSPO in microglia, macrophages and infiltrating CD4+ T lymphocytes, lasting until day 20.

Discussion of TSPO PET Radiotracer for Spinal Cord Imaging

An inflammatory response is present in several spinal cord pathologies. As argued above, this opens up many indications for the use of the TSPO PET radiotracer in spinal cord PET imaging. Five TSPO radiotracers have been described for spinal cord imaging, for MS (EAE model), NP (PSNL and CRPS models), spinal cord injury, ALS, and lumbar radiculopathy.

Overall, the TSPO PET radiotracer showed similar results: (1) capacity to detect spinal cord inflammatory processes; (2) capacity to evaluate treatment; and (3) correlation with histology and TSPO expression in microglia. Only [^{11}C]PK11195 and [^{18}F]DPA-714 showed mixed results for detecting lesions in the spinal cord compared to uninjured sites in neuropathic pain, although [^{18}F]DPA-714 showed higher lesion-to-background signal.[81] These mixed results were explained by the poor spatial resolution of PET, while ex-vivo and in-vitro studies showed significant results. However, in neuropathic pain, [^{18}F]GE-180 showed higher capacity to detect lesions on PET images.[86] [^{18}F]GE-180 is also known to have a higher lesion-to-background ratio; this has been largely discussed, and challenges the imaging characteristics of this radiotracer.[89-92] Further studies to compare these radiotracers are required.

This is especially interesting as most of these radiotracers could be used in clinical applications, but only [^{11}C]PBR28 has been used in a clinical study.[82] A translational study to compare each TSPO radiotracer to assess their potential in spinal cord PET imaging would be interesting.

Importantly, a polymorphism (Ala17Thr) was found for the TSPO gene and differentiates subjects as "high/mixed/low" affinity binders.[93] Some radiotracers are known to be sensitive to this polymorphism ([^{11}C]PBR28,[94] [^{18}F]GE-180,[95] and [^{18}F]DPA-714[96]) or their status is unknown ([^{11}C]DAC). In clinical studies to explore spinal cord TSPO radiotracers this question should be raised.

The choice of the TSPO PET radiotracer may also be guided by the radionuclide used for radiolabeling. For example, PK11195 and PBR28 are radiolabeled with carbon-11; its short half-life of 20 minutes restricts its use to medical centers equipped with an on-site cyclotron. Fluorine-18 radiotracers, with a longer half-life of 109 minutes, are more flexible and improve statistical measurement of radioactivity.

TSPO PET has several limitations in imaging the spinal cord. Firstly, TSPO is an ubiquitarian protein involved in many physiological mechanisms. Thus, it is nonspecific to any given pathology and could not differentiate an inflammatory process from various other spinal cord pathologies. Moreover, it is not known whether the uptake observed in various models is specific to spinal cord microglia or circulating macrophages.[97] Furthermore, the TSPO PET radiotracer also binds to surrounding organs such as bone marrow and muscles[98] and has a spill-over effect on the spinal cord signal. Ultimately, TSPO protein is a biomarker of the microenvironment of the spinal cord and not a direct biomarker of spinal cord integrity. Table 1 summarizes TSPO PET radiotracer characteristics used for spinal cord imaging.

Neurotransmission Radiotracers

Table 2 summarizes PET neurotransmission radiotracer characteristics used for spinal cord imaging.

[^{18}F]/[^{11}C]fallypride

[^{18}F]fallypride and [^{11}C]fallypride are dopamine D2/D3 receptor PET radiotracers. Kaur et al. reported fallypride[99] to image dopamine receptors along the spinal cord in rodents.

Table 1 TSPO PET Radiotracer Use in Spinal Cord Imaging

Radiotracer	Indication	Strengths	Limitations
[^{11}C]PK11195	MS	First TSPO radiotracer used for SC imaging	^{11}C radiolabeling
	SCI	Able to detect SC inflammation	TSPO not specific to spinal cord
	NP	Used to evaluate treatment	Mixed results in NP
		Correlation with clinical and histologic data	
		No sensitive to polymorphism	
[^{18}F]DPA-714	MS	Able to detect SC inflammation in MS	TSPO not specific to spinal cord
	ALS	Correlation with histology in MS	Mixed results in NP
	NP	Higher lesion-to-background ratio*	Sensitive to polymorphism
[^{11}C]PBR-28	LR	Clinical study	^{11}C radiolabeling
		Able to detect clinically significant differences	TSPO not specific to spinal cord
			Sensitive to polymorphism
[^{18}F]GE-180	SCI	Able to detect SC inflammation	TSPO not specific to spinal cord
	NP	Used to evaluate treatment	Sensitive to polymorphism
		Correlation with histology	
		Higher lesion-to-background ratio*	
[^{11}C]DAC	MS	Able to detect SC inflammation	^{11}C radiolabeling
		Correlation with histology	TSPO not specific to spinal cord
		Used to evaluate treatment	Sensitive to polymorphism

MS, multiple sclerosis; SC, spinal cord; SCI, spinal cord injury; NP, neuropathic pain; ALS, amyotrophic lateral sclerosis; LR, lumbar radiculopathy.

*compared to [^{11}C]PK11195.

Table 2 PET Neurotransmission Radiotracers for Spinal Cord Imaging

Target	Radiotracer	Indication	Strengths	Limitations
D2/D3R	[^{18}F]/[^{11}C]fallypride	Healthy subjects	Receptor expression quantifiable Specific binding confirmed	[^{18}F]fluorine binding due to metabolite Capacity to detect change unknown
GSA	[^{13}N]NH_3	SCI	Biomarker for BSCB integrity	^{13}N radiolabeling Low uptake at baseline Uptake after injury represents BSCB disruption Not specific to SC integrity
SERT	[^{11}C]AFM	SCI	Clinical studies (translational) Preclinical studies positive	^{11}C radiolabeling No or little specific binding in humans. Not able to detect clinical differences
SV2A	[^{11}C]UCB-J	HD SCI	Clinical studies (positive) Preclinical studies positive Superior to [^{18}F]FDG Specific binding Correlation with histology	^{11}C radiolabeling Several radiometabolite

HD, Huntington's disease; SCI, spinal cord injury.

[^{18}F]fallypride was first used for in-vitro and ex-vivo autoradiography studies. Then in-vivo and ex-vivo PET studies were performed using both [^{18}F]fallypride and [^{11}C]fallypride. Autoradiography studies showed preferential binding in gray matter in the superficial dorsal and dorsal horn. The gray/white matter ratio showed higher binding in higher spinal cord levels: cervical>thoracic>lumbar>sacral. Ex-vivo and PET studies revealed comparable binding in the spinal cord and extrastriatal brain regions. [^{18}F]fallypride and [^{11}C]fallypride showed similar binding curves. Several D2/D3 antagonists (sulpiride, clozapine, haloperidol) and agonists (dopamine) showed displacement in in-vitro binding assays, confirming specific binding. [^{11}C]fallypride was used to assess [^{18}F]fluoride binding on bones. Thus, differences with [^{18}F]fallypride were attributed to [^{18}F]fluoride binding on bones and spill-over effect.

[^{18}F] and [^{11}C]fallypride are valuable radiotracers for exploring dopamine neurotransmission in the spinal cord, since in-vivo and ex-vivo quantification showed binding comparable to other brain regions, such as the superior and inferior colliculi (around 5% striatal binding). Competition studies with agonists and antagonists also showed displacement of fallypride binding. This confirmed application to assess target engagement for future therapies targeting these receptors. The next step for this radiotracer will be to evaluate it in a spinal cord pathology. Kaur et al. proposed to explore D2/D3 receptors in restless leg syndrome.

[^{13}N]NH_3

[^{13}N]NH_3 is a PET radiotracer used for imaging glutamine synthetase activity, since glutamate and ammonia react to yield glutamine.[100] Usually used for cardiac and cerebral blood flow exploration, late-phase [^{13}N]NH_3 reflects [^{13}N]glutamine distribution. One study explored the use of late-phase [^{13}N]NH_3 to explore the spinal cord.[101] [^{13}N]NH_3 uptake was compared to [^{18}F]FDG uptake in a canine model of hemisection spinal cord injury. PET/CT was performed before and at days 1, 3, 7, 14 and 21 after surgery. After injury, both [^{13}N]NH_3 and [^{18}F]FDG showed increased uptake, with peaks at days 7 and 3 for [^{13}N]NH_3 and [^{18}F]FDG respectively. In parallel, brain uptake also increased for both radiotracers. MCP-1 chemokine and ZO-1 expression (anti-zonula occluden 1) were also measured to assess BSCB permeability. MCP-1 chemokine on ELISA increased at day 1 and reached a peak at day 7. ZO-1 expression was measured at day 21 by immunostaining and showed a slight but non-significant decrease in expression in dogs with spinal cord injury vs controls. A significant correlation was found between barrier integrity biomarkers and [^{13}N]NH_3 spinal cord uptake. This suggested BSCB disruption. These results also showed the lack of [^{13}N]NH_3 penetration compared to [^{18}F]FDG. Overall, [^{13}N]NH_3 seems not to be a valuable tool to explore the spinal cord but could be useful to assess the BSCB integrity.

[^{11}C]AFM

[^{11}C]AFM is a PET radiotracer targeting the serotonin transporter (SERT).[102] Two studies reported [^{11}C]AFM to image the spinal cord, one[103] with preliminary results for the second.[104] In the second translational study, 1 healthy male volunteer and two male patients with spinal cord injury (T4 and C5-C6 level) underwent whole-body PET scan. In a preclinical study, spinal cord injury rats underwent PET scan at 12 weeks postinjury and 12 weeks post-treatment. Control rats and rats with complete resection were imaged once. In-vivo competition study was performed using citalopram (SERT inhibitor) to assess specific binding of [^{11}C]AFM. In a preclinical study, PET images showed decreased lumbar uptake (below the injury point) while cervical uptake was maintained after injury. Citalopram competition study showed similar nonspecific binding between brain and spinal cord (around 35%). In humans, spinal cord PET images and competition study using citalopram showed no specific binding in the spinal cord. There were no differences in [^{11}C]AFM binding between cervical and lumbar levels in the two patients with spinal cord injury. [^{11}C]AFM also showed no change in spinal cord imaging after blocking with citalopram, which indicated little specific binding. There was even greater uptake in the pretreatment scan than baseline, possibly due to more peripheral or brain blocking than in the

spinal cord. Thus, [^{11}C]AFM seems not to be suited to image the spinal cord, except in preclinical models.

[^{11}C]UCB-J

[^{11}C]UCB-J is a PET radiotracer with high affinity for synaptic vesicle glycoprotein 2A (SV2A), a presynaptic protein regulating neurotransmitter release.[105] Three studies used [^{11}C]UCB-J to image the spinal cord: two preclinical in Huntington's disease and spinal cord injury,[106,107] and 1 clinical study in healthy humans.[108]

In the first study,[106] in-vivo PET/CT scans were performed in a wild-type and a knock-in Q175D mouse model of Huntington's disease and postmortem human Huntington's disease brains. Spinal cord [^{11}C]UCB-J uptake on cervical slices was lower in Q175D than in wild-type mice. Competition study using levetiracetam confirmed specific binding to SV2A. Postmortem study in human Huntington's disease brains [^{3}H]UCB-J showed lower uptake in patients than in controls.

In the second study,[107] [^{11}C]UCB-J was used as a biomarker of synapse loss after spinal cord injury. The model consisted in a unilateral C5 contusion in mice and rats. In a first in-vitro study, mouse and rat models of spinal cord injury were sacrificed 1 week after injury for histology (SV2A immunostaining) and autoradiography (using [^{3}H]UCB-J) to assess differences between species. This in-vitro study showed a sub-acute decrease in SV2A after spinal cord injury in both mice and rats. Immunostaining showed SV2A loss in epicenter of the impact point compared to the contralateral side ($F_{(1,24)} = 140.4$, $P < 0.0001$ in mice and $F_{(1,28)} = 20.2$, $P < 0.0001$ in rats) with an 80% decrease compared to rostral slices. Autoradiography results were consistent with these findings. In the second part, rats with wide spinal cords were chosen for longitudinal study. They underwent dynamic [^{11}C]UCB-J PET/CT scan at week 1 and week 6 after injury. Static [^{18}F]FDG PET/CT scan was also performed at week 6, to assess metabolic activity in the spinal cord. [^{11}C]UCB-J uptake was significantly lower in spinal cord injury than sham rats at the C5 contusion site. Uptake was also significantly (49%) lower at C5 (lesion point) than C3 (uninjured). This reduction at 1-week postinjury continued until 6 weeks and also induced a caudal loss of SV2A at C7. Comparing [^{18}F]FDG and [^{11}C]UCB-J profiles at week 6, [^{18}F]FDG showed hypometabolism at the contusion site compared to sham rats and surrounding tissues. The comparison was in favor of [^{11}C]UCB-J, with higher sensitivity. Histological and autoradiography studies were consistent with these findings and with the first part of the in-vitro study.

The third study explored [^{11}C]UCB-J binding in human spinal cord.[108] First, a simulation study was performed to assess the ability of [^{11}C]UCB-J to measure SV2A blocking. Second, cervical spinal cord imaging was performed in four healthy humans, at baseline and after pretreatment with levetiracetam or brivaracetam. Data were acquired using a high-resolution research tomograph (HRRT). Finally, human full spinal cord PET/CT imaging from previous dosimetry study (n = 4) was used to quantify spinal cord SV2A. Simulation study based on 75% brain occupancy calculated simulated V_T and V_{ND} volumes in the spinal cord. In the cervical spinal cord, on HRRT, nondisplaceable binding potential ($BP_{ND} = 0.43$) correlated strongly with the simulation study ($BP_{ND} = 0.43$), although mean estimated V_{ND} values were slightly lower than simulated V_{ND} (16%). Full spinal cord images showed less uptake in the spinal cord than in the brain (78 ± 5%). A simplified reference tissue model showed higher distribution volume ratio in cervical than thoracic slices (0.145 ± 0.051 and 0.112 ± 0.016 respectively). Estimated cervical spinal cord V_T was about 5% less than the baseline V_T reported for the human HRRT data.

[^{11}C]UCB-J seems to be a valuable radiotracer to image the spinal cord, detecting significant changes in the spinal cord in various preclinical models. It also showed promising capacity in a clinical modeling study using previous data acquired on various scans with various resolutions. Like other radiotracers, [^{11}C]UCB-J is radiolabeled with carbon-11, which limits its clinical use and impairs PET image quality due to greater noise. SV2A radiolabeled with fluorine-18, such as [^{18}F]SynVesT-1, could be more interesting.[109] Finally, [^{11}C]UCB-J was reported to have several radiometabolites which did not cross the blood-brain barrier.[110] However, further studies are needed to determine whether they could cross the BSCB and thus compromise the spinal cord PET signal.

Myelin-Specific Radiotracers

[^{11}C]MeDAS

[^{11}C]MeDAS is a PET radiotracer to image myelination.[111] It was used in three studies to image spinal cord demyelination.[77,112,113] Wu et al. used [^{11}C]MeDAS to monitor myelin repair in the spinal cord in two models of MS: a lysophosphatidyl choline (LPC) model of focal demyelination, and EAE.[112] PET/CT scans were performed on days 7, 14 and 21 for LPC rats and days 0 and at the first three disease episodes for EAE rats. LPC rats were separated in two subgroups: treated (hepatocyte growth factor) and untreated (saline). In LPC rats, [^{11}C]MeDAS PET images showed the lowest uptake at day 7, at peak demyelination. Uptake gradually increased, by 22% and 28% respectively, at days 14 and 21 in the T11-T12 region, due to remyelination. These results correlated with myelin spinal cord staining in in-vitro studies. LPC-treated rats showed greater [^{11}C]MeDAS uptake in the spinal cord compared to control rats. At days 14 and 21, LPC-treated rats showed respectively 31% and 14% increase in uptake compared to day 7. Results were confirmed by immunohistochemical analysis of spinal cord myelination. In the EAE group, [^{11}C]MeDAS showed decreased uptake in T10-T13 spinal cord at days 15, 25 and 42 after induction compared to baseline. Results correlated with EAE disability score.

De Paula Faria et al. also used [^{11}C]MeDAS in a rat EAE model.[77] Rats underwent PET/CT at baseline and days 6, 11, 15 and 19 after induction. In contrast to Wu et al.'s findings, they did not show significant demyelination using [^{11}C]MeDAS PET images. However, histochemistry showed small lesions (0.13 ± 0.06 mm). The authors stated that poor

spatial resolution in the camera and differences in lesion level (lumbar and thoracic) prevented results being significant.

In a third study, [^{11}C]MeDAS was compared to another myelin PET radiotracer, [^{11}C]CIC, in a model of cuprizone-induced demyelination.[113] Mice underwent PET/CT imaging and ex-vivo biodistribution study. The study focused on brain uptake but, due to the PET characteristics of the tracers, [^{11}C]MeDAS is preferentially used for spinal cord imaging. In-vivo images showed significant background uptake for [^{11}C]CIC, leading to a low brain-to-background ratio. Moreover, [^{11}C]CIC showed weak correlation with histochemistry analysis of myeline ($r^2 = 0.15$), probably due to a spill-over effect. [^{11}C]CIC also showed slow washout of the radiotracer. Longer brain accumulation led to longer acquisition time, which could be problematic for a radiotracer radiolabeled with carbon-11. Finally, [^{11}C]CIC was not able to visualize the spinal cord in in-vivo images. In contrast, [^{11}C]MeDAS showed less background uptake and thus a better ratio, facilitating visualization of myelin in the brain and spinal cord. [^{11}C]MeDAS also showed fast kinetics, allowing rapid acquisition after injection, but with lower SUV values complicating detection of differences. [^{11}C]MeDAS PET imaging correlated with histochemistry.

[^{18}F]TAFDAS

[^{18}F]TAFDAS is a 1, 2 ,3-triazole fluorinated derivate of [^{11}C]MeDAS. One study explored its use in spinal cord imaging.[114] In this preliminary study, Wu et al. acquired exploratory PET/CT images of rat spinal cord to assess the ability of [^{18}F]TAFDAS to detect spinal cord demyelination. In a model of spinal cord injury, [^{18}F]TAFDAS PET images showed markedly lower uptake (0.81 vs 1.02) in injured than preinjury T13 slices. Uptake in T13 was also lower than in other thoraco-lumbar slices. In situ 3D cryoimaging staining using unlabeled TAFDAS coregistered with PET/CT images confirmed this result and showed demyelination in the dorsal region. This multimodal technique combined the high sensitivity of physiological information and quantification provided by PET and microscopic information provided by 3D histological cryoimaging.

[^{18}F]PENDAS

[^{18}F]PENDAS is a derivate of [^{11}C]MeDAS, assessed as a PET radiotracer in spinal cord imaging in one study.[115] In a series of stilbene derivatives, [^{18}F]PENDAS was chosen for its lipophilic and radiolabeling properties, fluorescence and specificity to myelin. In-vivo PET/CT imaging of the spinal cord showed higher uptake for [^{18}F]PENDAS than [^{11}C]MeDAS or [^{18}F]TAFDAS. A rat model of spinal cord injury (contusion at T12) showed 14% lower [^{18}F]PENDAS uptake than in other nontraumatic thoracic regions. In-situ histological staining confirmed these results and showed a decrease in the dorsal column. Ex-vivo 3D cryofluorescence imaging after PET/CT allowed coregistration and facilitated spatial orientation.

Discussion of Myelin PET Radiotracers

[^{11}C]MeDAS was the first original PET radiotracer to image myelin and to monitor treatment response.[112] However, it gave inconsistent results in PET spinal cord imaging, as described above, attributed to smaller lesion sizes than camera resolution. Enhancement of imaging techniques and higher resolution could help to overcome this issue. Another limitation is radiolabeling using carbon-11, which limits clinical use to centers equipped with an on-site cyclotron. Derivates were therefore synthesized to be radiolabeled with fluorine-18. Thus, TAFDAS and PENDAS were chosen from around 20 compounds, based on their lipophilic and radiolabeling properties. These compounds also allow multimodal imaging with 3D cryofluorescence and show excellent correlation with PET/CT images. In spinal cord PET imaging, [^{18}F]TAFDAS and [^{18}F]PENDAS were able to detect spinal cord lesions in models of spinal cord injury. However, these preliminarily results need to be further explored in larger samples, and to be compared with controls.

Notably, some amyloid radiotracers with a stilbene structure similar to myelin radiotracers, such as [^{18}F]florbetapir and [^{18}F]florbetaben, were reported to target myelin and repurposed to image myelin, but only in the brain.[116] Studies showed interesting results, with decreased binding of amyloid radiotracers in white matter in patients with multiple sclerosis.[117,118] These studies did not show whether it was able to detect lesions in the spinal cord. To our knowledge, no such studies have been reported, but are needed to test this hypothesis. Table 3 summarizes characteristics of myelin PET radiotracers used for spinal cord imaging.

Table 3 PET Myelin Radiotracers for Spinal Cord Imaging

Radiotracer	Indication	Strengths	Limits
[^{11}C]MeDAS	MS	Multimodality	^{11}C radiolabeling
		Correlation with histology	Inconsistent results between studies
		Correlation with clinical symptoms in rats	
		Low background signal	
[^{18}F]TAFDAS	SCI	Multimodality	Insufficient data
		Able to detect lesion	
[^{18}F]PENDAS	SCI	Multimodality	Insufficient data
		Higher uptake in SC (compared to myelin radiotracers)	
		Able to detect lesion	

MS, multiple sclerosis; SC, spinal cord; SCI, spinal cord injury.

Others

[18F]FSPG

[18F]FSPG is a PET radiotracer of cystine/glutamate antiporter (system xc−) with applications in cancer [119] and neurology.[120] Release of glutamate by system xc− was reported to be involved in microglia and macrophage activation in MS.[121] Thus, one study explored the use of [18F]FSPG to image the spinal cord in an EAE model of MS.[122] PET/CT scans were performed at days 0 (baseline), 7, 14, 21 and 28 after EAE induction. One group received [11C]PK1195 and [18F]FDG to assess TSPO binding and glucose metabolism, and a second group received [18F]FSPG to assess system xc− binding. PET images of glucose metabolism showed nonsignificant postoperative hypometabolism in the thoracic spinal cord, cervical and lumbar levels showing similar binding at every time point. [11C]PK11195 spinal cord PET images showed an increase in radiotracer uptake until day 14, followed by a decrease from day 21 to 28. [18F]FSPG showed higher binding values in the spinal cord than in brain regions at baseline. Cervical and thoracic spinal cord slices showed nonsignificant decrease in binding at day 7 and recovery at days 14 and 28, whereas lumbar slices showed significantly higher uptake values at day 14 and a decrease from day 21 to 28. Immunohistochemistry and clodronate effect studies confirmed microglia activation and correlation with system xc- after EAE induction.

In this study, [18F]FDG showed a lack of sensitivity for detecting inflammatory MS in the spinal cord. In-vivo TSPO PET confirmed previous findings of the ability of [11C]PK11195 to detect inflammatory spinal cord response in EAE rats.[74,77] [18F]FSPG showed a different binding profile than [11C]PK11195. This could be explained by different microglial/macrophage populations. [18F]FSPG showed its ability to evaluate EAE progression in the spinal cord and discriminate spinal cord lesion severity at different levels, in correlation with paralysis symptoms. This novel radiotracer provides a different opportunity to image the spinal cord in MS and a new tool for therapy evaluation. Table 4 summarizes the characteristics of [18F]FSPG used for spinal cord imaging.

[11C]TZ3321

[11C]TZ3321 is a sphingosine-1-phosphate receptor 1 (S1PR1) PET radiotracer.[123] One study reported [11C]TZ3321 to image the spinal cord in an EAE rat model of MS.[124] EAE rats, with scores of 3.5-4.0 on a neurological deficit scoring system,[79] underwent PET/CT. Asymptomatic age-matched sham rats also underwent PET/CT as controls. Normalized SUV ratio, with the abdominal aorta as reference region, showed 24.6% higher [11C]TZ3321 uptake in the lumbar spinal cord of EAE rats than for the sham group. Distribution volume ratio using the Logan reference model showed similar results, with an increase of 22.5% in EAE rats. Histological analysis showed an increase in S1PR1 rates in EAE rats expressed in activated microglia and astrocytes. The number of interleukin-17-producing T cells was also higher in EAE rat spinal cord, and colocalized with S1PR1 expression. These results confirmed the correlation between S1PR1 expression and neuroinflammation of the lumbar spinal cord in the EAE model. [11C]TZ3321 is a valuable PET radiotracer for in-vivo exploration of S1PR1 expression in the spinal cord and thus for assessing neuroinflammatory response. Modeling analysis was possible thanks to the abdominal aorta reference region that was similar between EAE and sham control rats. Table 4 summarizes the characteristics of [11C]TZ3321 used for spinal cord imaging.

Perspectives

Several PET radiotracers are in development to explore various spinal cord pathologies (see summary in Fig. 1). As a conclusion, we highlight the characteristics of the "ideal" PET radiotracer for imaging the spinal cord. Firstly, it must cross the BSCB. Then, it must have little nonspecific binding, notably in surrounding tissues such as bone marrow. This characteristic allows low doses for patients and a better lesion-to-background ratio. The radiotracer must have good sensitivity for detecting micro-changes in the spine. The choice of the radionuclide is also important. Fluorine-18, with its longer half-life, is more suitable for clinical practice. However, after metabolization, free fluorine-18 could be captured by the bones, adding to noise and spill-over.

Independently of the radiotracer itself, the choice of target is also important. The more specific the target to the spinal cord, the more the radiotracer reflects a specific disease process. Depending on the disease, the target must be expressed all along the spine. The characteristics of the radiotracer

Table 4 Other PET Radiotracers in Spinal Cord Imaging

Target	Radiotracer	Indication	Strengths	Limits
System xc−	[18F]FSPG	MS	Higher SC binding compared to brain Able to detect lesion Used to evaluate treatment Correlation with histology Different profile than TSPO radiotracer	
S1PR1	[11C]TZ3321	MS	Able to detect lesion Correlation with histology Modeling study with reference region	11C radiolabeling

MS: multiple sclerosis.

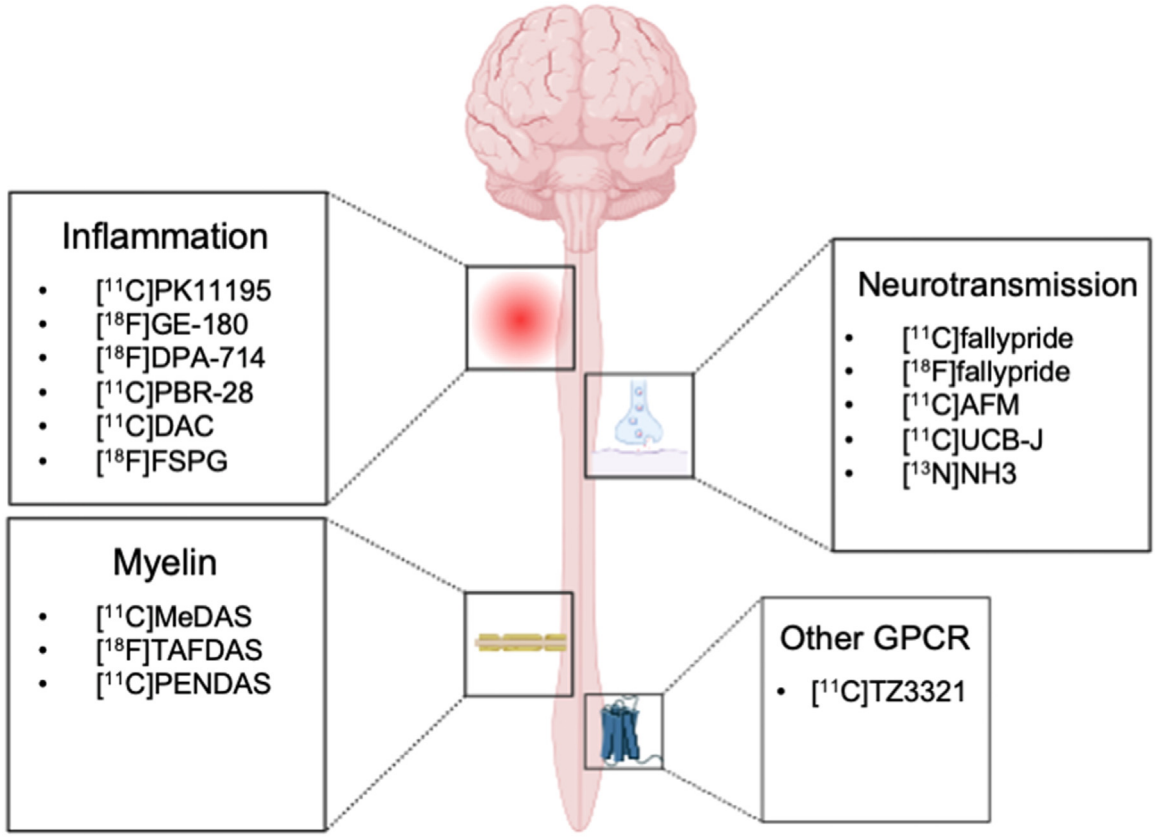

Figure 1 Summary of radiotracers used for functional PET imaging of the spinal cord. GPCR, G protein-coupled receptors.

must be explored in a large cohort to determine the influence of factors such age or body weight on binding. Finally, for clinical practice, a market authorization ensures access for all nuclear medicine centers. For multicenter studies, a standardized acquisition and quantification protocol is needed.

In a multimodal approach, the choice of camera is important. Nuclear medicine centers usually have easier access to a PET/CT camera. However, the interest of PET-MR camera could be discussed. Since MRI could be the first-line choice for spinal cord imaging, a PET-MR camera could be interesting, reducing the number of scanning procedures. PET-MRI combines the high sensitivity of MRI and the molecular information of PET imaging. Compared to PET/CT, it has the advantage that MRI does not involve radiation. Furthermore, MRI provides better soft-tissue contrast and multiparametric and functional information, with diffusion-weighted and dynamic sequences, spectroscopy, etc. Since it is more widespread, most studies used PET/CT. However, hybrid PET-MRI seems to be more suitable, as it acquires both modalities at same time, improving coregistration. MRI is also more suitable for visualizing contours between bone tissues and soft tissues. Aiello et al. showed the feasibility of PET-MR spinal cord imaging in comparison with PET/CT.[71]

The development of PET radiotracers and improvements to clinical PET cameras will enable information to be acquired at molecular level in the spinal cord. This will help for diagnosis and also for better understanding of spinal cord diseases, search for new targets and development of new drugs. Altogether, PET spinal cord imaging has a promising future as a complement to MRI and CT.

Declaration of competing interest

The authors declare that they have no known competing financial interests or personal relationships that could have appeared to influence the work reported in this paper.

CRediT authorship contribution statement

Pierre Courault: Conceptualization, Methodology, Writing – original draft. **Luc Zimmer:** Conceptualization, Methodology, Supervision, Writing – review & editing. **Sophie Lancelot:** Supervision, Validation, Writing – review & editing.

References

1. Bican O, Minagar A, Pruitt AA: The spinal cord. Neurol Clin 31(1): 1-18, 2013. https://doi.org/10.1016/j.ncl.2012.09.009
2. Dale N, Roberts A: Dual-component amino-acid-mediated synaptic potentials: excitatory drive for swimming in Xenopus embryos. J Physiol 363(1):35-59, 1985. https://doi.org/10.1113/jphysiol.1985.sp015694

3. Curtis DR, Hösli L, Johnston GAR: A pharmacological study of the depression of spinal neurones by glycine and related amino acids. Exp Brain Res 6(1):1-18, 1968.. https://doi.org/10.1007/BF00235443
4. Scullion K, Boychuk JA, Yamakawa GR, et al: Serotonin 1A receptors alter expression of movement representations. J Neurosci 33 (11):4988-4999, 2013. https://doi.org/10.1523/JNEUROSCI.4241-12.2013
5. Levant B, McCarson KE: D3 dopamine receptors in rat spinal cord: implications for sensory and motor function. Neurosci Lett 303(1):9-12, 2001. https://doi.org/10.1016/S0304-3940(01)01692-5
6. Garraway SM, Hochman S: Modulatory actions of serotonin, norepinephrine, dopamine, and acetylcholine in spinal cord deep dorsal horn neurons. J Neurophysiol 86(5):2183-2194, 2001. https://doi.org/10.1152/jn.2001.86.5.2183
7. Henry JL, Krnjević K, Morris ME: Substance P and spinal neurones. Can J Physiol Pharmacol 53(3):423-432, 1975. https://doi.org/10.1139/y75-061
8. Harmann PA, Chung K, Briner RP, et al: Calcitonin gene-related peptide (CGRP) in the human spinal cord: a light and electron microscopic analysis. J Comp Neurol 269(3):371-380, 1988. https://doi.org/10.1002/cne.902690305
9. Kang Y, Ding H, Zhou H, et al: Epidemiology of worldwide spinal cord injury: a literature review. J Neurorestoratology 6:1-9, 2017. https://doi.org/10.2147/JN.S143236
10. Goldberg AL, Kershah SM: Advances in imaging of vertebral and spinal cord injury. J Spinal Cord Med 33(2):105-116, 2010. https://doi.org/10.1080/10790268.2010.11689685
11. Wang TY, Park C, Zhang H, et al: Management of acute traumatic spinal cord injury: a review of the literature. Front Surg 8:698736. https://doi.org/10.3389/fsurg.2021.698736, 2021
12. Howard J, Trevick S, Younger DS: Epidemiology of multiple sclerosis. Neurol Clin 34(4):919-939, 2016. https://doi.org/10.1016/j.ncl.2016.06.016
13. Trapp BD, Nave KA: Multiple sclerosis: an immune or neurodegenerative disorder? Annu Rev Neurosci 31(1):247-269, 2008. https://doi.org/10.1146/annurev.neuro.30.051606.094313
14. Brownlee WJ, Hardy TA, Fazekas F, et al: Diagnosis of multiple sclerosis: progress and challenges. The Lancet 389(10076):1336-1346, 2017. https://doi.org/10.1016/S0140-6736(16)30959-X
15. Thompson AJ, Banwell BL, Barkhof F, et al: Diagnosis of multiple sclerosis: 2017 revisions of the McDonald criteria. Lancet Neurol 17 (2):162-173, 2018. https://doi.org/10.1016/S1474-4422(17)30470-2
16. Hauser SL, Cree BAC: Treatment of multiple sclerosis: a review. Am J Med 133(12):1380-1390.e2, 2020. https://doi.org/10.1016/j.amjmed.2020.05.049
17. Talbott EO, Malek AM, Lacomis D: The epidemiology of amyotrophic lateral sclerosis. *Handbook of Clinical Neurology*. Vol 138. Radarweg 29, 1043 NX Amsterdam, The Netherlands: Elsevier B.V., 225-238. https://doi.org/10.1016/B978-0-12-802973-2.00013-6, 2016
18. Kiernan MC, Vucic S, Cheah BC, et al: Amyotrophic lateral sclerosis. The Lancet 377(9769):942-955, 2011. https://doi.org/10.1016/S0140-6736(10)61156-7
19. Lenglet T, Camdessanché JP: Amyotrophic lateral sclerosis or not: keys for the diagnosis. Rev Neurol (Paris) 173(5):280-287, 2017. https://doi.org/10.1016/j.neurol.2017.04.003
20. Bensimon G, Lacomblez L, Meininger V: A controlled trial of riluzole in amyotrophic lateral sclerosis. N Engl J Med 330(9):585-591, 1994. https://doi.org/10.1056/NEJM199403033300901
21. Abe K, Aoki M, Tsuji S, et al: Safety and efficacy of edaravone in well defined patients with amyotrophic lateral sclerosis: a randomised, double-blind, placebo-controlled trial. Lancet Neurol 16(7):505-512, 2017. https://doi.org/10.1016/S1474-4422(17)30115-1
22. Chenaf C, Delorme J, Delage N, et al: Prevalence of chronic pain with or without neuropathic characteristics in France using the capture−recapture method: a population-based study. Pain 159(11):2394-2402, 2018. https://doi.org/10.1097/j.pain.0000000000001347
23. Cavalli E, Mammana S, Nicoletti F, et al: The neuropathic pain: An overview of the current treatment and future therapeutic approaches. Int J Immunopathol Pharmacol 33:205873841983838. https://doi.org/10.1177/2058738419838383, 2019
24. A novel gene containing a trinucleotide repeat that is expanded and unstable on Huntington's disease chromosomes. The Huntington's Disease Collaborative Research Group. Cell 72(6):971-983, 1993. https://doi.org/10.1016/0092-8674(93)90585-e
25. Pringsheim T, Wiltshire K, Day L, et al: The incidence and prevalence of Huntington's disease: a systematic review and meta-analysis. Mov Disord 27(9):1083-1091, 2012. https://doi.org/10.1002/mds.25075
26. Margolis RL, Ross CA: Diagnosis of huntington disease. Clin Chem 49 (10):1726-1732, 2003. https://doi.org/10.1373/49.10.1726
27. Cruickshank TM, Reyes AP, Penailillo LE, et al: Effects of multidisciplinary therapy on physical function in Huntington's disease. Acta Neurol Scand 138(6):500-507, 2018. https://doi.org/10.1111/ane.13002
28. Grimstvedt TN, Miller JU, van Walsem MR, et al: Speech and language difficulties in Huntington's disease: a qualitative study of patients' and professional caregivers' experiences. Int J Lang Commun Disord 56 (2):330-345, 2021. https://doi.org/10.1111/1460-6984.12604
29. Frank S: Treatment of Huntington's Disease. Neurotherapeutics 11 (1):153-160, 2014. https://doi.org/10.1007/s13311-013-0244-z
30. Sciacca G, Cicchetti F: Mutant huntingtin protein expression and blood−spinal cord barrier dysfunction in huntington disease. Ann Neurol 82(6):981-994, 2017. https://doi.org/10.1002/ana.25107
31. Tarulli AW, Raynor EM: Lumbosacral radiculopathy. Neurol Clin 25 (2):387-405, 2007. https://doi.org/10.1016/j.ncl.2007.01.008
32. Berry JA, Elia C, Saini HS, et al: A review of lumbar radiculopathy, diagnosis, and treatment. Cureus 11:1-17, 2019. https://doi.org/10.7759/cureus.5934. Published online
33. Stochkendahl MJ, Kjaer P, Hartvigsen J, et al: National Clinical Guidelines for non-surgical treatment of patients with recent onset low back pain or lumbar radiculopathy. Eur Spine J Off Publ Eur Spine Soc Eur Spinal Deform Soc Eur Sect Cerv Spine Res Soc 27(1):60-75, 2018. https://doi.org/10.1007/s00586-017-5099-2
34. Freund P, Seif M, Weiskopf N, et al: MRI in traumatic spinal cord injury: from clinical assessment to neuroimaging biomarkers. Lancet Neurol 18(12):1123-1135, 2019. https://doi.org/10.1016/S1474-4422(19)30138-3
35. Lycklama G, Thompson A, Filippi M, et al: Spinal-cord MRI in multiple sclerosis. Lancet Neurol 2(9):555-562, 2003. https://doi.org/10.1016/S1474-4422(03)00504-0
36. Pierre-Jerome C, Arslan A, Bekkelund SI: MRI of the spine and spinal cord: imaging techniques, normal anatomy, artifacts, and pitfalls. J Manipulative Physiol Ther 23(7):470-475, 2000. https://doi.org/10.1067/mmt.2000.108819
37. Stroman PW, Wheeler-Kingshott C, Bacon M, et al: The current state-of-the-art of spinal cord imaging: methods. NeuroImage 84:1070-1081, 2014. https://doi.org/10.1016/j.neuroimage.2013.04.124
38. Vedantam A, Jirjis MB, Schmit BD, et al: Diffusion tensor imaging of the spinal cord: insights from animal and human studies. Neurosurgery 74(1):1-8, 2014. https://doi.org/10.1227/NEU.0000000000000171. discussion 8; quiz 8
39. Moffett J, Ross B, Arun P, et al: N-Acetylaspartate in the CNS: from neurodiagnostics to neurobiology. Prog Neurobiol 81(2):89-131, 2007. https://doi.org/10.1016/j.pneurobio.2006.12.003
40. Barry RL, Vannesjo SJ, By S, et al: Spinal cord MRI at 7T. NeuroImage 168:437-451, 2018. https://doi.org/10.1016/j.neuroimage.2017.07.003
41. Vargas MI, Boto J, Meling TR: Imaging of the spine and spinal cord: an overview of magnetic resonance imaging (MRI) techniques. Rev Neurol (Paris) 177(5):451-458, 2021. https://doi.org/10.1016/j.neurol.2020.07.005
42. Urrutia J, Cuellar J, Zamora T: Spondylolysis and spina bifida occulta in pediatric patients: prevalence study using computed tomography as a screening method. Eur Spine J Off Publ Eur Spine Soc Eur Spinal Deform Soc Eur Sect Cerv Spine Res Soc 25(2):590-595, 2016. https://doi.org/10.1007/s00586-014-3480-y
43. Shah LM, Ross JS: Imaging of spine trauma. Neurosurgery 79(5):626-642, 2016. https://doi.org/10.1227/NEU.0000000000001336

44. Kornblum MB, Wesolowski DP, Fischgrund JS, et al: Computed tomography-guided biopsy of the spine. A review of 103 patients. Spine 23(1):81-85, 1998. https://doi.org/10.1097/00007632-199801010-00018
45. Da Ros V, Picchi E, Ferrazzoli V, et al: Spinal vascular lesions: anatomy, imaging techniques and treatment. Eur J Radiol Open 8:100369. https://doi.org/10.1016/j.ejro.2021.100369, 2021
46. Kiamanesh Z, Banezhad F, Nasiri Z, et al: Physiological distribution of 18F-FDG in the spinal cord: a systematic review. J Spinal Cord Med 44(4):517-524, 2021. https://doi.org/10.1080/10790268.2019.1672954
47. Wilmshurst JM, Barrington SF, Pritchard D, et al: Positron emission tomography in imaging spinal cord tumors. J Child Neurol 15(7):465-472, 2000. https://doi.org/10.1177/088307380001500708
48. Nguyen NC, Sayed MM, Taalab K, et al: Spinal cord metastases from lung cancer: detection with F-18 FDG PET/CT. Clin Nucl Med 33(5):356-358, 2008. https://doi.org/10.1097/RLU.0b013e31816a784c
49. Mapelli P, Vanoli EG, Picchio M, et al: Spinal cord involvement secondary to non-Hodgkin's lymphoma identified by 18F-FDG PET/CT. Rev Esp Med Nucl E Imagen Mol 32(2):125, 2013. https://doi.org/10.1016/j.remn.2012.10.009
50. Shen G, Ma H, Pan L, et al: FDG PET/CT and MRI in primary spinal cord glioblastoma. Clin Nucl Med 45(3):e144-e145, 2020. https://doi.org/10.1097/RLU.0000000000002800
51. Flanagan EP, Hunt CH, Lowe V, et al: [18F]-fluorodeoxyglucose—positron emission tomography in patients with active myelopathy. Mayo Clin Proc 88(11):1204-1212, 2013. https://doi.org/10.1016/j.mayocp.2013.07.019
52. Schmitz A, Risse JH, Textor J, et al: FDG-PET findings of vertebral compression fractures in osteoporosis: preliminary results. Osteoporos Int 13(9):755-761, 2002. https://doi.org/10.1007/s001980200103
53. Bredella MA, Essary B, Torriani M, et al: Use of FDG-PET in differentiating benign from malignant compression fractures. Skeletal Radiol 37(5):405-413, 2008. https://doi.org/10.1007/s00256-008-0452-5
54. He X, Zhao L, Guo X, et al: Differential diagnostic value of ^{18}F-FDG PET/CT for benign and malignant vertebral compression fractures: comparison with magnetic resonance imaging. Cancer Manag Res 10:2105-2115, 2018. https://doi.org/10.2147/CMAR.S168374
55. Zhou X, Cipriano P, Kim B, et al: Detection of nociceptive-related metabolic activity in the spinal cord of low back pain patients using ^{18} F-FDG PET/CT. Scand J Pain 15(1):53-57, 2017. https://doi.org/10.1016/j.sjpain.2016.11.017
56. Ota K, Tsunemi T, Saito K, et al: 18F-FDG PET successfully detects spinal cord sarcoidosis. J Neurol 256(11):1943-1946, 2009. https://doi.org/10.1007/s00415-009-5270-8
57. Ordóñez-Rubiano EG, Solano-Noguera DF, Row W, et al: Dual timepoint 18F-FDG PET/CT in spinal sarcoidosis: a single institution case series. Spine 44(21):E1248-E1255, 2019. https://doi.org/10.1097/BRS.0000000000003122
58. Nandoe Tewarie RDS, Yu J, Seidel J, et al: Positron emission tomography for serial imaging of the contused adult rat spinal cord. Mol Imaging 9(2):108-116, 2010
59. von Leden RE, Selwyn RG, Jaiswal S, et al: 18F-FDG-PET imaging of rat spinal cord demonstrates altered glucose uptake acutely after contusion injury. Neurosci Lett 621:126-132, 2016. https://doi.org/10.1016/j.neulet.2016.04.027
60. Kindred JH, Koo PJ, Rudroff T: Glucose uptake of the spinal cord in patients with multiple sclerosis detected by 18F-fluorodeoxyglucose PET/CT after walking. Spinal Cord 52(S3):S11-S13, 2014. https://doi.org/10.1038/sc.2014.130
61. Marini C, Cistaro A, Campi C, et al: A PET/CT approach to spinal cord metabolism in amyotrophic lateral sclerosis. Eur J Nucl Med Mol Imaging 43(11):2061-2071, 2016. https://doi.org/10.1007/s00259-016-3440-3
62. Emsen B, Fitoussi A, Chalaye J, et al: FDG PET/CT of cervical gout with spinal cord compression. Clin Nucl Med 45(1):e29-e31, 2020. https://doi.org/10.1097/RLU.0000000000002772
63. Taralli S, Leccisotti L, Mattoli MV, et al: Physiological activity of spinal cord in children: an 18F-FDG PET-CT study. Spine 40(11):E647-E652, 2015. https://doi.org/10.1097/BRS.0000000000000895
64. Gupta V: Positron emission tomography in spinal cord disease. Mayo Clin Proc 88(11):1188-1190, 2013. https://doi.org/10.1016/j.mayocp.2013.09.004
65. Sahel OA, Bazine A, Nabih SO, et al: Unsuspected intramedullary spinal cord metastasis detected by FDG PET/CT. Indian J Nucl Med IJNM Off J Soc Nucl Med India 35(4):353-354, 2020. https://doi.org/10.4103/ijnm.IJNM_150_20
66. Kelloff GJ, Hoffman JM, Johnson B, et al: Progress and promise of FDG-PET imaging for cancer patient management and oncologic drug development. Clin Cancer Res 11(8):2785-2808, 2005. https://doi.org/10.1158/1078-0432.CCR-04-2626
67. Kamoto Y, Sadato N, Yonekura Y, et al: Visualization of the cervical spinal cord with FDG and high-resolution PET. J Comput Assist Tomogr 22(3):487-491, 1998. https://doi.org/10.1097/00004728-199805000-00023
68. Aliyev A, Saboury B, Kwee TC, et al: Age-related inflammatory changes in the spine as demonstrated by (18)F-FDG-PET:observation and insight into degenerative spinal changes. Hell J Nucl Med 15(3):197-201, 2012. https://doi.org/10.1967/s002449910054
69. Amin A, Rosenbaum SJ, Bockisch A: Physiological 18F-FDG uptake by the spinal cord: is it a point of consideration for cancer patients? J Neurooncol 107(3):609-615, 2012. https://doi.org/10.1007/s11060-011-0785-0
70. Schwab JH, Healey JH: FDG-PET lacks sufficient sensitivity to detect myxoid liposarcoma spinal metastases detected by MRI. Sarcoma 2007:1-3, 2007. https://doi.org/10.1155/2007/36785
71. Aiello M, Alfano V, Salvatore E, et al: [18F]FDG uptake of the normal spinal cord in PET/MR imaging: comparison with PET/CT imaging. EJNMMI Res 10(1):91, 2020. https://doi.org/10.1186/s13550-020-00680-8
72. Shah F, Hume SP, Pike VW, et al: Synthesis of the enantiomers of [N-methyl-11C]PK 11195 and comparison of their behaviours as radioligands for PK binding sites in rats. Nucl Med Biol 21(4):573-581, 1994. https://doi.org/10.1016/0969-8051(94)90022-1
73. Chauveau F, Becker G, Boutin H: Have (R)-[11C]PK11195 challengers fulfilled the promise? A scoping review of clinical TSPO PET studies. Eur J Nucl Med Mol Imaging 49(1):201-220, 2021. https://doi.org/10.1007/s00259-021-05425-w
74. Vowinckel E, Reutens D, Becher B, et al: PK11195 binding to the peripheral benzodiazepine receptor as a marker of microglia activation in multiple sclerosis and experimental autoimmune encephalomyelitis. J Neurosci Res 50(2):345-353, 1997. https://doi.org/10.1002/(SICI)1097-4547(19971015)50:2<345::AID-JNR22>3.0.CO;2-5
75. Banati RB, Newcombe J, Gunn RN, et al: The peripheral benzodiazepine binding site in the brain in multiple sclerosis: quantitative in vivo imaging of microglia as a measure of disease activity. Brain J Neurol 123(Pt 11):2321-2337, 2000. https://doi.org/10.1093/brain/123.11.2321
76. Karchewski LA, Bloechlinger S, Woolf CJ: Axonal injury-dependent induction of the peripheral benzodiazepine receptor in small-diameter adult rat primary sensory neurons. Eur J Neurosci 20(3):671-683, 2004. https://doi.org/10.1111/j.1460-9568.2004.03530.x
77. de Paula Faria D, Vlaming MLH, Copray SCVM, et al: PET imaging of disease progression and treatment effects in the experimental autoimmune encephalomyelitis rat model. J Nucl Med Off Publ Soc Nucl Med 55(8):1330-1335, 2014. https://doi.org/10.2967/jnumed.114.137216
78. Imamoto N, Momosaki S, Fujita M, et al: [11C]PK11195 PET imaging of spinal glial activation after nerve injury in rats. NeuroImage 79:121-128, 2013. https://doi.org/10.1016/j.neuroimage.2013.04.039
79. Abourbeh G, Theze B, Maroy R, et al: Imaging microglial/macrophage activation in spinal cords of experimental autoimmune encephalomyelitis rats by positron emission tomography using the mitochondrial 18 kDa translocator protein radioligand [18F]DPA-714. J Neurosci 32

(17):5728-5736, 2012. https://doi.org/10.1523/JNEUROSCI.2900-11.2012
80. Gargiulo S, Anzilotti S, Coda ARD, et al: Imaging of brain TSPO expression in a mouse model of amyotrophic lateral sclerosis with 18F-DPA-714 and micro-PET/CT. Eur J Nucl Med Mol Imaging 43 (7):1348-1359, 2016. https://doi.org/10.1007/s00259-016-3311-y
81. Shimochi S, Keller T, Kujala E, et al: Evaluation of [18F]F-DPA PET for detecting microglial activation in the spinal cord of a rat model of neuropathic pain. Mol Imaging Biol 24:641-650, 2022.. https://doi.org/10.1007/s11307-022-01713-5. Published online
82. Albrecht DS, Ahmed SU, Kettner NW, et al: Neuroinflammation of the spinal cord and nerve roots in chronic radicular pain patients. Pain 159(5):968-977, 2018. https://doi.org/10.1097/j.pain.0000000000001171
83. Wadsworth H, Jones PA, Chau WF, et al: [18F]GE-180: a novel fluorine-18 labelled PET tracer for imaging translocator protein 18kDa (TSPO). Bioorg Med Chem Lett 22(3):1308-1313, 2012. https://doi.org/10.1016/j.bmcl.2011.12.084
84. Fan Z, Calsolaro V, Atkinson RA, et al: Flutriciclamide (^{18}F-GE180) PET: first-in-human PET study of novel third-generation in vivo marker of human translocator protein. J Nucl Med 57(11):1753-1759, 2016. https://doi.org/10.2967/jnumed.115.169078
85. Tremoleda JL, Thau-Zuchman O, Davies M, et al: In vivo PET imaging of the neuroinflammatory response in rat spinal cord injury using the TSPO tracer [18F]GE-180 and effect of docosahexaenoic acid. Eur J Nucl Med Mol Imaging 43(9):1710-1722, 2016. https://doi.org/10.1007/s00259-016-3391-8
86. Cropper HC, Johnson EM, Haight ES, et al: Longitudinal translocator protein-18 kDa—positron emission tomography imaging of peripheral and central myeloid cells in a mouse model of complex regional pain syndrome. Pain 160(9):2136-2148, 2019. https://doi.org/10.1097/j.pain.0000000000001607
87. Yanamoto K, Yamasaki T, Kumata K, et al: Evaluation of N-benzyl-N-[11C]methyl-2- (7-methyl-8-oxo-2-phenyl-7,8-dihydro-9H-purin-9-yl)acetamide ([11C]DAC) as a novel translocator protein (18 kDa) radioligand in kainic acid-lesioned rat. Synap N Y N 63(11):961-971, 2009. https://doi.org/10.1002/syn.20678
88. Xie L, Yamasaki T, Ichimaru N, et al: [(11)C]DAC-PET for noninvasively monitoring neuroinflammation and immunosuppressive therapy efficacy in rat experimental autoimmune encephalomyelitis model. J Neuroimmune Pharmacol Off J Soc NeuroImmune Pharmacol 7(1):231-242, 2012. https://doi.org/10.1007/s11481-011-9322-3
89. Zanotti-Fregonara P, Veronese M, Pascual B, et al: The validity of 18F-GE180 as a TSPO imaging agent. Eur J Nucl Med Mol Imaging 46 (6):1205-1207, 2019. https://doi.org/10.1007/s00259-019-4268-4
90. Albert NL, Unterrainer M, Brendel M, et al: In response to: the validity of 18F-GE180 as a TSPO imaging agent. Eur J Nucl Med Mol Imaging 46(6):1208-1211, 2019. https://doi.org/10.1007/s00259-019-04294-8
91. Zanotti-Fregonara P, Veronese M, Rizzo G, et al: Letter to the editor re: confirmation of specific binding of the 18-kDa translocator protein (TSPO) radioligand [18F]GE-180: a blocking study using XBD173 in multiple sclerosis normal appearing white and grey matter. Mol Imaging Biol 22(1):10-12, 2020. https://doi.org/10.1007/s11307-019-01433-3
92. Nicholas R, Brooks D, Owen D: In Response to letter from fregonara et al. 2019. Mol Imaging Biol 22(1):13-14, 2020. https://doi.org/10.1007/s11307-019-01463-x
93. Owen DR, Yeo AJ, Gunn RN, et al: An 18-kDa translocator protein (TSPO) polymorphism explains differences in binding affinity of the PET radioligand PBR28. J Cereb Blood Flow Metab 32(1):1-5, 2012. https://doi.org/10.1038/jcbfm.2011.147
94. Owen DRJ, Gunn RN, Rabiner EA, et al: Mixed-affinity binding in humans with 18-kDa translocator protein ligands. J Nucl Med Off Publ Soc Nucl Med 52(1):24-32, 2011. https://doi.org/10.2967/jnumed.110.079459
95. Vettermann FJ, Harris S, Schmitt J, et al: Impact of TSPO receptor polymorphism on [18F]GE-180 binding in healthy brain and pseudoreference regions of neurooncological and neurodegenerative disorders. Life 11(6):484, 2021. https://doi.org/10.3390/life11060484
96. Lavisse S, García-Lorenzo D, Peyronneau MA, et al: Optimized quantification of translocator protein radioligand ^{18} F-DPA-714 uptake in the brain of genotyped healthy volunteers. J Nucl Med 56(7):1048-1054, 2015. https://doi.org/10.2967/jnumed.115.156083
97. Cosenza-Nashat M, Zhao ML, Suh HS, et al: Expression of the translocator protein of 18 kDa by microglia, macrophages and astrocytes based on immunohistochemical localization in abnormal human brain. Neuropathol Appl Neurobiol 35(3):306-328, 2009. https://doi.org/10.1111/j.1365-2990.2008.01006.x
98. Gent YYJ, Voskuyl AE, Kloet RW, et al: Macrophage positron emission tomography imaging as a biomarker for preclinical rheumatoid arthritis: findings of a prospective pilot study. Arthritis Rheum 64(1):62-66, 2012. https://doi.org/10.1002/art.30655
99. Kaur J, Kharajian A, Coleman RA, et al: Spinal cord dopamine D2/D3 receptors: in vivo and ex vivo imaging in the rat using 18F/11C-fallypride. Nucl Med Biol 41(10):841-847, 2014. https://doi.org/10.1016/j.nucmedbio.2014.08.002
100. Momosaki S, Ito M, Tonomura M, et al: Assessment of glutamine synthetase activity by [13N]ammonia uptake in living rat brain. Synap N Y N 69(1):26-32, 2015. https://doi.org/10.1002/syn.21781
101. Zhang L, López-Picón FR, Jia Y, et al: Longitudinal [18F]FDG and [13N]NH3 PET/CT imaging of brain and spinal cord in a canine hemisection spinal cord injury model. NeuroImage Clin 31:102692. https://doi.org/10.1016/j.nicl.2021.102692, 2021
102. Huang Y, Hwang DR, Bae SA, et al: A new positron emission tomography imaging agent for the serotonin transporter: synthesis, pharmacological characterization, and kinetic analysis of [11C]2-[2-(dimethylaminomethyl)phenylthio]-5-fluoromethylphenylamine ([11C]AFM). Nucl Med Biol 31(5):543-556, 2004. https://doi.org/10.1016/j.nucmedbio.2003.11.008
103. Wang X, Duffy P, McGee AW, et al: Recovery from chronic spinal cord contusion after Nogo receptor intervention. Ann Neurol 70(5):805-821, 2011. https://doi.org/10.1002/ana.22527
104. Fang H, Rossano S, Wang X, et al: Translational PET imaging of spinal cord injury with the serotonin transporter tracer [11C]AFM. Mol Imaging Biol 24:560-569, 2022.. https://doi.org/10.1007/s11307-021-01698-7. Published online
105. Nabulsi NB, Mercier J, Holden D, et al: Synthesis and preclinical evaluation of 11C-UCB-J as a PET tracer for imaging the synaptic vesicle glycoprotein 2A in the brain. J Nucl Med Off Publ Soc Nucl Med 57 (5):777-784, 2016. https://doi.org/10.2967/jnumed.115.168179
106. Bertoglio D, Verhaeghe J, Wyffels L, et al: Synaptic vesicle glycoprotein 2A is affected in the CNS of Huntington's Disease mice and postmortem human HD brain. J Nucl Med Off Publ Soc Nucl Med 63:942-947, 2021. https://doi.org/10.2967/jnumed.121.262709. Published online:jnumed.121.262709
107. Bertoglio D, Halloin N, De Lombaerde S, et al: SV2A PET imaging is a non-invasive marker for the detection of spinal damages in experimental models of spinal cord injury. J Nucl Med 63:1245-1251, 2022. https://doi.org/10.2967/jnumed.121.263222. Published online: jnumed.121.263222
108. Rossano S, Toyonaga T, Bini J, et al: Feasibility of imaging synaptic density in the human spinal cord using [11C]UCB-J PET. EJNMMI Phys 9(1):32, 2022. https://doi.org/10.1186/s40658-022-00464-0
109. Li S, Cai Z, Wu X, et al: Synthesis and *in Vivo* evaluation of a novel pet radiotracer for imaging of synaptic vesicle glycoprotein 2A (SV2A) in nonhuman primates. ACS Chem Neurosci 10(3):1544-1554, 2019. https://doi.org/10.1021/acschemneuro.8b00526
110. Finnema SJ, Nabulsi NB, Mercier J, et al: Kinetic evaluation and test—retest reproducibility of [^{11} C]UCB-J, a novel radioligand for positron emission tomography imaging of synaptic vesicle glycoprotein 2A in humans. J Cereb Blood Flow Metab 38(11):2041-2052, 2018. https://doi.org/10.1177/0271678X17724947
111. Wu C, Wang C, Popescu DC, et al: A novel PET marker for in vivo quantification of myelination. Bioorg Med Chem 18(24):8592-8599, 2010. https://doi.org/10.1016/j.bmc.2010.10.018
112. Wu C, Zhu J, Baeslack J, et al: Longitudinal positron emission tomography imaging for monitoring myelin repair in the spinal cord. Ann Neurol 74(5):688-698, 2013. https://doi.org/10.1002/ana.23965

113. de Paula Faria D, de Vries EFJ, Sijbesma JWA, et al: PET imaging of demyelination and remyelination in the cuprizone mouse model for multiple sclerosis: a comparison between [11C]CIC and [11C]MeDAS. NeuroImage 87:395-402, 2014. https://doi.org/10.1016/j.neuroimage.2013.10.057
114. Wu C, Eck B, Zhang S, et al: Discovery of 1,2,3-triazole derivatives for multimodality PET/CT/cryoimaging of myelination in the central nervous system. J Med Chem 60(3):987-999, 2017. https://doi.org/10.1021/acs.jmedchem.6b01328
115. Tiwari AD, Zhu J, You J, et al: Novel 18F-labeled radioligands for positron emission tomography imaging of myelination in the central nervous system. J Med Chem 62(10):4902-4914, 2019. https://doi.org/10.1021/acs.jmedchem.8b01354
116. Auvity S, Tonietto M, Caillé F, et al: Repurposing radiotracers for myelin imaging: a study comparing 18F-florbetaben, 18F-florbetapir, 18F-flutemetamol,11C-MeDAS, and 11C-PiB. Eur J Nucl Med Mol Imaging 47(2):490-501, 2020. https://doi.org/10.1007/s00259-019-04516-z
117. Matías-Guiu JA, Cabrera-Martín MN, Matías-Guiu J, et al: Amyloid PET imaging in multiple sclerosis: an 18F-florbetaben study. BMC Neurol 15(1):243, 2015. https://doi.org/10.1186/s12883-015-0502-2
118. Zhang M, Ni Y, Zhou Q, et al: 18F-florbetapir PET/MRI for quantitatively monitoring myelin loss and recovery in patients with multiple sclerosis: a longitudinal study. eClinicalMedicine 37:100982. https://doi.org/10.1016/j.eclinm.2021.100982, 2021
119. Baek S, Choi CM, Ahn SH, et al: Exploratory clinical trial of (4 *S*)-4-(3-[^{18} F]fluoropropyl)-l-glutamate for imaging x $_{C}$ $^{-}$ transporter using positron emission tomography in patients with non−small cell lung or breast cancer. Clin Cancer Res 18(19):5427-5437, 2012. https://doi.org/10.1158/1078-0432.CCR-12-0214
120. Soria FN, Pérez-Samartín A, Martin A, et al: Extrasynaptic glutamate release through cystine/glutamate antiporter contributes to ischemic damage. J Clin Invest 124(8):3645-3655, 2014. https://doi.org/10.1172/JCI71886
121. Pampliega O, Domercq M, Soria FN, et al: Increased expression of cystine/glutamate antiporter in multiple sclerosis. J Neuroinflammation 8:63, 2011. https://doi.org/10.1186/1742-2094-8-63
122. Martín A, Vázquez-Villoldo N, Gómez-Vallejo V, et al: In vivo imaging of system xc- as a novel approach to monitor multiple sclerosis. Eur J Nucl Med Mol Imaging 43(6):1124-1138, 2016. https://doi.org/10.1007/s00259-015-3275-3
123. Jin H, Yang H, Liu H, et al: A promising carbon-11-labeled sphingosine-1-phosphate receptor 1-specific PET tracer for imaging vascular injury. J Nucl Cardiol Off Publ Am Soc Nucl Cardiol 24(2):558-570, 2017. https://doi.org/10.1007/s12350-015-0391-1
124. Liu H, Jin H, Yue X, et al: PET imaging study of S1PR1 expression in a rat model of multiple sclerosis. Mol Imaging Biol 18(5):724-732, 2016. https://doi.org/10.1007/s11307-016-0944-y